THE PENNSYLVANIA STATE UNIVERSITY
SCHREYER HONORS COLLEGE

DEPARTMENT OF ASTRONOMY AND ASTROPHYSICS

# THE ENVIRONMENTS OF LUMINOUS BLUE VARIABLES AND THE LINK TO THE ENIGMATIC TYPE IIN SUPERNOVAE

COLE PENKUNAS
SPRING 2024

A thesis
submitted in partial fulfillment
of the requirements
for baccalaureate degrees
in Astronomy & Astrophysics and Physics
with honors in Astronomy & Astrophysics

Reviewed and approved* by the following:

Abe Falcone
Associate Professor of Astronomy and Astrophysics
Thesis Supervisor

Stein Sigurdsson
Professor of Astronomy and Astrophysics
Honors Adviser

*Signatures are on file in the Schreyer Honors College.

# Abstract

Using H$\alpha$ images of nearby galaxies and the normalized cumulative ranking pixel statistics method, we undertook the largest analysis of the environments of luminous blue variables (LBVs) with respect to regions of ongoing star formation (SF) in their respective host galaxies as traced by H$\alpha$ emission. We also compared the distribution of LBVs to the distribution of type IIn supernovae (SNe IIn) as a means of exploring the latter's possible progenitors. The scale of our study was achieved with the creation of the first continuum subtracted H$\alpha$ composite image of the entire M 31 galaxy. We analyzed the LBVs by comparing the distribution of candidate and confirmed LBVs to regions of H$\alpha$ emission in their host galaxies. We then ranked the location of each LBV and candidate LBV (cLBV) in the form of a normalized cumulative rank (NCR) to determine how well each sample traced H$\alpha$ emission in the galaxies studied. Additionally, we utilized radial analysis to analyze the locations of LBVs and cLBVs in relation to their hosts' light distribution in the R and H$\alpha$ bands. We find that confirmed LBVs trace regions of ongoing SF well, while our candidate sample does not. These differences suggest that LBVs are a subset of cLBVs, but cLBVs are not a subset of LBVs. Finally, we find that confirmed LBVs are consistent with sharing a parent population distribution with the non-zero NCR SN IIn population, suggesting that confirmed LBVs make up a significant portion of the progenitors of SNe IIn in regions of ongoing SF.

# Table of Contents

# List of Figures

# List of Tables

# Chapter 1

# Introduction

Luminous Blue Variables (LBVs) are a rare class of massive, luminous stars characterized by large, long-lasting outbursts and variable visual brightness, along with their titular typical blue color. Long periods of greatly increased visual brightness (sometimes several magnitudes' difference) lasting many years have been observed in stars such as $\eta$ Car, P Cyg, and S Dor, but it was not until 1984 that these variations were linked to each other and the new class of star was coined [17].

One of the defining features of LBVs is that, while their visual brightness greatly changes between periods of outburst and quiescence, their bolometric luminosity seems to stay constant. The exact mechanism for these outbursts (which can vary in periodicity, timescale, and degree of brightening) is still being debated (see Section 1.2 and Smith [76]). The other interesting feature of LBVs is the inferred mass-loss that occurs sporadically during outbursts and regularly due to the strong stellar winds, leaving large quantities of ejecta that forms the surrounding circumstellar medium (CSM) [41]. LBVs have been inferred to lose large portions of their mass in outbursts over their lifetime, such as in AG Car, which lost 25 $M_\odot$ of its initial $65$ $M_\odot$ [84]. Additionally, massive eruptions have been observed, such as the the Great Eruption of $\eta$ Car in 1843 [77]. These eruptions are large enough to be mistaken as supernovae, such as the supernova (SN) imposter SN 2009ip [6] (which did eventually evolve into a true SNe IIn in 2012 [60]).

## 1.1 "Traditional" view of SNe IIn

The aforementioned ejecta that forms the CSM are of particular interest as a proposed progenitor of type IIn supernovae (SNe IIn), a relatively rare class of SNe that makes up only around 5% of observed type II SNe [15]. SNe IIn are a heterogeneous class (see Section 1.2) of SNe typically considered as core-collapse supernovae (CCSNe) with narrow spectral features on the H Balmer lines (especially H$\alpha$), as well as an early blue continuum and a slow spectroscopic evolution [74] [68]. The observed H Balmer line profiles are complex, with multiple components stemming from various possible interactions. There is also an observed narrow component (FWHM on the order

of 200 kms$^{-1}$) that may be due to interaction with a dense, H-rich CSM [23]. Additionally, there are typically broader H$\alpha$ and H$\beta$ lines present, attributed to broad lines from the ejecta [11], as well as strong, smooth wings attributed to electron-scattering winds in the circumstellar shell [10].

LBVs are also the only confirmed progenitor of SNe IIn, after the progenitor of SN 2005gl was identified as a high mass ($> 60M_{\odot}$) LBV with archival HST images [25][24] and the SN imposter SN 2009ip (which was in reality an LBV outburst) evolved into a genuine SNe IIn [9]. Efforts are underway to better understand the link between SNe IIn and LBVs. As the CSM shell has been shed by the progenitor, LBVs that have undergone violent mass loss episodes are consistent with being a possible progenitor for SNe IIn due to the envelope they shed during their outbursts [71]. While the specific mechanisms at work are an active area of research, further observations seem to support this relationship: Smith [76] argues that SN 2009ip, SN 2011ht, and possibly SN 1961V are very strong candidates to have LBV progenitors due to precursor interactions, further supporting the theory of LBVs as (at least one of the) progenitors of SNe IIn. More recent studies, however, have suggested that LBVs may not be the only progenitors of the type.

## 1.2 Problems with "traditional" SNe IIn

In recent years, the overall validity of the SN IIn class has been called into question. Although SNe IIn as a group was initially clearly defined, many similar (but not quite the same) SNe have been since identified and categorized (sometime erroneously) as SNe IIn. This may be caused by the heterogeneity of the category and subsequent difficulties in maintaining clear definitions for the class; the peak luminosity of SNe IIn, while typically very luminous (average peak $M_V$ = -18.4 mags [51]) can differ by more than two orders of magnitude. Additionally, the only truly "signature" feature of the class is their interaction with a dense CSM, which causes the observed narrow lines [62]. This heterogeneity has led to many other types of SNe being misclassified as SNe IIn in the past, further complicating efforts to solidly classify transients as SNe IIn.

Ransome et al. [68] recently undertook a reclassification of 115 objects historically classified as SNe IIn on public catalogues, and found that many were either only loosely "confirmed" SNe IIn or were altogether misclassified. Of the 115 candidates analyzed, only 37 were classified as 'gold,' showing clear CSM interaction over several epochs. 50 SNe IIn were classified as 'silver,' exhibiting CSM interaction or spectra consistent with the category, but without long enough or repeated observations necessary to be firmly classified as SNe IIn (as the developing spectrum may prove a mis-categorized to be another type of transient, such as a gap transient of SNe Ia-CSM, or has not yet developed the characteristic features). The remaining 28 objects were classified as non-SNe IIn, not showing enough features consistent with the rest of the category.

Additionally, the spatial distribution of SNe IIn has also generated questions about the class, specifically in respect to their progenitors. In a a survey of the environments of known SNe (both types I and II), James & Anderson [46] used a novel pixel statistics method (discussed further in Section 3.4) to compare the locations of SNe to regions of H$\alpha$ emission (an indicator of ongoing star formation) in their host galaxies. They found that, while CCSNe as a whole closely trace H$\alpha$ emission, the SNe II were not distributed "perfectly" (or uniformly) in regions of ongoing star formation (SF) as would be expected of high mass stars. This finding seemed to go against the conventional model for type of IIb and IIn SNe, where a young, massive progenitor is assumed.

Anderson et al. [5] followed up on James & Anderson [46] with another survey using the same method, and additionally analyzed archival data for regions of near-UV emission in the hosts. While regions of H$\alpha$ emission trace ongoing ($< 16$ Myr) SF well, regions of near-UV emissions are better associated with recent (16-100 Myr) SF [49] [27]. They found that $<$50% of surveyed SNe IIn were located in regions of ongoing SN, implying a progenitor older (and presumably less massive) than other types of SN II, or multiple progenitor paths for the type. Habergham et al. [33], using the same method, also found that the environments of known SNe IIn differ from those of SNe Ic, which are believed to have massive progenitors. SNe Ic were found to be uniformly trace H$\alpha$ emission, as predicted for transients with massive progenitors. A more recent study also found that, as a whole, SNe IIn are not well associated with ongoing SF, but of the individual SNe

IIn surveyed that *are* found near regions of H$\alpha$ emission, the distribution is as predicted for SNe with young, massive progenitors [69]. This could suggest that LBV progenitors might make a subset of SNe IIn that do trace SF as predicted (for the population of SNe IIn surveyed with non-zero cumulative reduced H$\alpha$ emission), while there may be other progenitor routes for the type. Curiously, though, SN 2009ip, a misclassified supernova that was later identified as a violent LBV "imposter" eruption (similar to the Great Eruption of $\eta$ Car) Berger et al. [6], but later evolved into a "true" SN IIn in 2012 [60], was found in a region with no H$\alpha$ emission. This represents a case of a presumed LBV (and subsequent SN IIn) in a place of little to no ongoing SF, a finding that goes against the traditional understanding of LBVs.

## 1.3 The "traditional" understanding of LBVs

Traditionally, LBVs are thought to be highly luminous, hot, evolved supergiants that are particularly unstable. They experience irregular outburst that cause great variability of visual brightness (called S Dor-type variations after the historical LBV), while their bolometric luminosity stays the same. LBVs also occasionally suffer giant eruptions (seen in $\eta$ Car and P Cyg), although these are rarer than the smaller, less volatile outbursts. During outbursts, a "pseudo-photosphere", an optically thick shell, may form in optically thick winds as the temperature of the star decreases, causing a reallocation of energy on the spectra and the dramatic change in visual brightness while the bolometric luminosity stays the same. In quiescence, LBVs can be found on the diagonal "S Dor Instability Strip" of the Hertzsprung-Russell diagram (HR diagram), while in outburst they shift rightward to a cooler (but just as luminous) vertical column in the HR diagram [41] [76]. This is shown in Figure 1.1, which is taken from Humphreys & Davidson [41] with permission.

While there is a lack of certainty in the literature for the exact mechanics that cause the instability, it was generally considered that LBVs' close proximity to the Eddington limit (due in part to a high L/M ratio from mass-loss during the main-sequence phase) leads to violent instability in the star. The instability and outbursts of the star lead to it shedding its H envelope over time, eventually

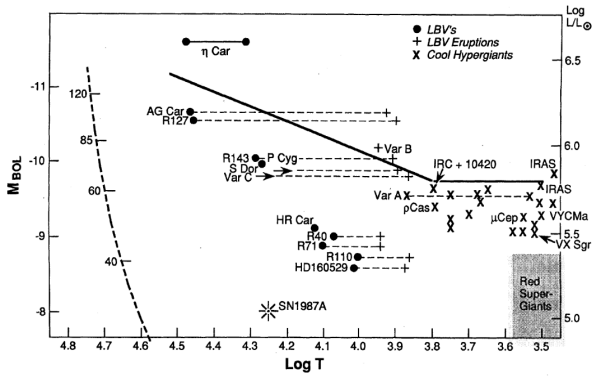


Figure 1.1: HR diagram including some the most luminous stars, including LBVs. The transition from quiescence (black dot) to outburst (called eruption here, black plus) is shown by the dashed lines. Schematic taken from Humphreys & Davidson [41] with permission.

evolving from the original O-type, main sequence (MS) star to an H-deficient Wolf-Rayet (WR) star [54].

There have also been observed LBVs of lower bolometric luminosity than is typical, such as R 71 in the Large Magellanic Cloud (LMC). Their eruptions display less magnitude and temperature variation, and are theorized to possibly have an alternate evolutionary path. However, their exact mechanics (like larger, "classical" LBVs) has not been well developed [41].

An LBV-like evolutionary stage has also been predicted by models of non-rotating, 60 $M_{\odot}$ main-sequence stars in Groh et al. [32]. They found that such a star begins producing LBV spectra in the last 10% of their MS. In the models, the star phased between hot and cool LBV stages as it first finished burning its H-core, before burning through its H-shell. It then began He-core burning and eventually evolved to a WNh type star (a WR still burning H in its core). However, while the non-rotating, 60 $M_{\odot}$ model was in line with traditional models of LBVs as evolutionary "stepping stones" for massive stars, the models in Groh et al. [31] predicted that rotating, 20-25 $M_{\odot}$ stars can appear as LBVs for a brief period (on the scale of $5000$ years) of He-core burning, before going SN in its LBV state. This model of less massive, less luminous LBVs may be consistent with the lower-luminosity population discussed by Humphreys & Davidson [41], and could possibly help address some of the issues with the "traditional" evolutionary view of LBVs.

## 1.4 Problems with "traditional" LBVs

Although some models support the "traditional" evolutionary path of LBVs, multiple problems arise from this classification. Chiefly amongst them is that the more luminous, traditional LBVs (as opposed to the ones found in Groh et al. [31]) cannot go SN before evolving to WR stars using current models [76] (as there would be no star left to evolve into a WR). While LBVs may not be the only (or even main) progenitor of SNe IIn, as mentioned in Section 1.2, there is at least one observed case of an LBV progenitor for a SN IIn in SN 2005gl. Additionally, the LBV outburst of SN 2009ip (which was misclassified as a SN) evolved to a genuine supernova in 2012 [60]. These cases pose an obvious problem for the classical models, as some observations do not agree with the aforementioned canonical models.

LBVs may also have a distribution issue, if the traditional explanation is assumed. Smith & Tombleson [78] found that a large fraction of known and LBV candidates are isolated from O-type stars. Candidate LBVs (cLBVs) are stars that share spectral properties with LBVs, but have not yet been observed in outburst [7]. If LBVs are a "transition" stage of massive O-type stars, one would expect their distribution in host-galaxies to be explicitly correlated with O-star clusters. However, the LBVs and cLBVs investigated were rarely found in star clusters, and of the ones that were, the star clusters were significantly older than would be expected for O-type stars. Furthermore, the study also found that the LBVs and cLBVs were more isolated from O-type stars than WR stars were. If the basic evolution proceeds as

$$O - type \rightarrow LBV \rightarrow WR,$$

one would expect the distribution of LBVs to be in between that of O-type and WR stars. This suggests the evolutionary process of at least some LBVs is still unclear (see Section 1.5 for proposed alternative evolutionary paths).

It should be noted that Davidson et al. [19] argued against some of the selection criteria used by

Smith & Tombleson [78], such as the use of candidates in their analysis, as well as pointing out that the luminous, "classical" LBVs investigated are well-associated with O-type stars, as predicted. However, Smith [76] argued that the cLBVs had no statistical difference in their environments, making any error in the selection criteria statistically meaningless in that regard. Additionally, even for the group of "classical" LBVs associated with O-type stars, the association was only with late O-type stars, which are not luminous enough to be in line to support the "traditionally" assumed distribution. On top of this, definitively differentiating distinct populations of LBVs (as discussed by Humphreys & Davidson [41]), or even categorizing the boundaries of LBVs as a whole on the HR diagram, remains incredibly difficult, given the small number of confirmed LBVs [13].

In addition to the possible distribution/age issue, the proposed mechanics for the formation of LBVs and the root causes of the instability and outbursts are disputed. The "pseudo-photosphere" that was proposed as the cause of the brightness changes during S Dor outbursts are not able to occur naturally in models of LBVs with realistic wind structures [20], nor were simulated pseudo-photospheres consistent with observations over longer periods of time [2]. Gräfener et al. [29] also found that the LBV AG Car, contrary to the literature, showed changes in bolometric luminosity between minimum and maximum V-band brightness (a finding supported by Groh et al. [30]). The study found, specifically, that the amount of "lost energy" from the changes in bolometric luminosity was the same as the energy needed to expand the radius of AG Car and inflate its envelope during an outburst. In their models, it was found that a hot, optically thick wind below the outer envelope (as would be present in the proposed "pseudo-photosphere" model) would reach outflow velocities that would affect the structure of an inflated envelope found by Petrovic et al. [66]. In this case, the wind would be strong enough to overcome gravity and reach a critical mass-loss rate that would inhibit sustaining an inflated envelope. However, in a recent study of 1,000 observed very massive stars in the VLT-Flames Tarantula Survey, Gräfener [28] predicted 20 LBVs in a population synthesis based on current evolutionary models using the proposed envelope inflation, but no LBVs or LBV-like objects were found in the survey itself. This argues against the envelope-inflation explanation, at least for conventional, H burning LBVs, as the observations did

not match the simulation (though it was noted that the mechanism could still occur in hypothetical fast-rotating LBVs as explored in Groh et al. [31] or in very late-stage, pre-SN evolutionary stages).

## 1.5 Proposed alternative LBV model

One alternative model of LBVs initially proposed by Kenyon & Gallagher III [50] and elaborated upon more recently by Smith [76] is a binary evolution. This evolutionary model starts with two less massive O-type stars evolving off the main sequence, and undergoing a binary merger or mass transfer. In the mass transfer scenario, the "gainer" would be overluminous for their location amongst surrounding stars, could become rapidly rotating due to the interaction, and may become enriched with the products of CNO burning. This model matches observations of both LBVs' overluminosity compared to their region [78] as well as observed chemical abundances around LBVs [18]. Additionally, CC SNe were only predicted in fast-rotating models of LBVs by [31], which can be potentially explain the observed LBV progenitors of SNe IIn if the LBVs were "spun up" by mass transfer interactions. All of these effects could occur in a binary merger as well.

Aghakhanloo et al. [3] investigated a binary evolutionary model as well, prompted by the findings of Smith & Tombleson [78]. The study found that if a binary pair was massive to start with (more massive than the pairs considered by Smith [76]), the mass gainer undergoing SN would provide sufficient mass and a large enough "kick" for the surviving companion to be launched out of its region of formation. The velocities reached from such a kick were found to be sufficient to cause an isolation from young, O-Type stars (the pair's place of birth) consistent with the findings of Smith & Tombleson [78] before the star died out.

Although a binary model would not be unprecedented, as over 70% of massive stars show signs of mass-exchange with a companion [72], recent attempts as supporting (or dismissing it) by looking for binary companions of known LBVs have failed [61]. Additionally, the model may only be accurate in describing the evolution of certain LBVs, such as the lower luminosity LBVs discussed by Humphreys & Davidson [41]. In particular, one of the chief complaints of Humphreys

et al. [42] with Smith & Tombleson [78] was that many of the data suggesting LBVs' isolation were from the least luminous LBVs, suggesting that they may have a different spatial distribution from "classical" LBVs (and thus, much of the motivation for a new model may only apply to these less luminous LBVs).

## 1.6 This study

The purpose of this study is to examine the environments of LBVs and cLBVs by looking at H$\alpha$ emission via the normalized cumulative rank (NCR) pixel statistics method described in James & Anderson [46] and discussed in Section 3.4. As mentioned previously, H$\alpha$ emission is well-associated with ongoing SF, so LBV's association with regions of H$\alpha$ correlate to their association with regions of ongoing SF and young, massive stars as a whole. In this study, we aim to shed light on the possible distribution issues discussed by Smith & Tombleson [78], as well as providing evidence for their locations in relation to regions of young, massive stars in their host galaxies.

Kangas et al. [48] present a similar study which used the same method to investigate the environments of proposed CC SNe progenitors (including LBVs) in the LMC and Messier 33. However, this study will focus solely on LBVs and cLBVs and use a larger sample size than their 14 total confirmed and candidate LBVs investigated between the two galaxies. Using the pixel statistics method will also allow a better direct comparison with the environments of SNe IIn as surveyed by Ransome et al. [69] using the same method, investigating the role of LBVs as progenitors for SNe IIn.

To improve on previous studies using the NCR pixel statistics method, we will be conducting the first analysis of LBVs in M 31 using this method. No previous study has performed the NCR pixels statistics method on M 31 before, as there was no prior existing continuous continuum reduced H$\alpha$ image of the entirety of the galaxy due to its massive angular size.

In addition to using the pixel statistics method to compare the environments LBVs and SNe IIn, we will also use radial analysis to compare the distribution of LBVs and SNe IIn in their respective

host galaxies. This is discussed further in Section 3.5.

# Chapter 2

# Data

Table 2.1: Sources for the R-band images and the distances, position angles, and eccentricities of the hosts used in radial anaysis.

| Host | R-band Image Source | Position Source |
|---|---|---|
| SMC | [8] | [22] |
| LMC | [8] | [22] |
| M 33 | [38] | [64] |
| IC 10 | [57] | [75] |

## 2.1 Host images

We used archival H$\alpha$ images of eight nearby galaxies to find regions of H II and thus ongoing SF. H$\alpha$ images of NGC 266 and NGC 2403 are our own images from the Liverpool telescope, while NGC 4736 was taken from [53], IC 10 from [21], and M 33 from [37]. M 31, which took up several separate fields, was taken from [56] and mosaiced. We then continuum subtracted these images (discussed in Section 3.1) for analysis. Already continuum subtracted images of the Small Magellanic Cloud (SMC) and Large Magellanic Cloud (LMC) were taken from [26].

The sources for the R-band images of hosts and the sources for their distances, position angles, and eccentricities are summarized in Table 2.1.

## 2.2 LBV catalogues

The catalogues of LBVs and cLBVs used for this study were taken from [58], [59], [1], [44], and [78]. Additionally, we analyzed the environment of NGC 4736_1, an individual LBV identified in [79], as well as SN 2005gl, which has a progenitor identified as an LBV by [25]. In this study, we differentiate between candidate (cLBVs) and well-established LBVs and defer to the classifications given by the reference(s) listed for each cLBV or LBV. In total, we use a sample of 23 confirmed LBVs and 84 candidates in our study.

# Chapter 3

# Methodology

## 3.1 Continuum Subtraction

Prior to our pixel statistics analysis, we transformed each H$\alpha$ image (other than those from Gaustad et al. [26]) by continuum subtracting the image. In order to use H$\alpha$ emission to properly map regions of ongoing SF in each galaxy, the excess R-band light that overlaps the H$\alpha$ filter range must first be removed. To do this, we first aligned and combined three H$\alpha$ exposures of the host galaxy. Then, with an R-band image of the galaxy, we used common, unsaturated stars to scale the R-band image to the H$\alpha$ images. After scaling, we subtracted the R-band light from the combined H$\alpha$ images, leaving a continuum subtracted H$\alpha$ image. This was accomplished with IRAF, AstroImageJ, and python.

Using this method, star artifacts are sometimes left over. This is an inherent drawback of the method due to difference in point spread functions between stars in each band. The images were not adjusted for a matched point spread function due to the effective degradation in the image artificially spreading out H$\alpha$ emission regions being inappropriate for our pixel statistics technique. This was particularly true for some regions of M 31's background (see Section 3.3). To minimize this problem, we masked noticeable star artifacts, discussed further in Section 3.4.

This process was altered for M 31, for which no H$\alpha$ image of the entire galaxy was available due to the galaxy's large angular isophotal size of 6200$''$ x 3478$''$ [47]. Because of the nature of pixel statistics providing only relative measurements, we required the entire galaxy in one image to properly perform the method (see Section 3.4). Due to this, we continuum subtracted separate fields of M 31 before mosaicing the resultant images together, the process described in Section 3.3.

## 3.2 Degradation of galaxies with resolved LBVs

Due to the high spatial resolution of some large, nearby galaxies, cLBVs and LBVs were resolved in some of our fields (an example of this is shown in Figure 3.1). Since the purpose of the our pixel statistics method (described in Section 3.4) is to rank the relative strength of emission

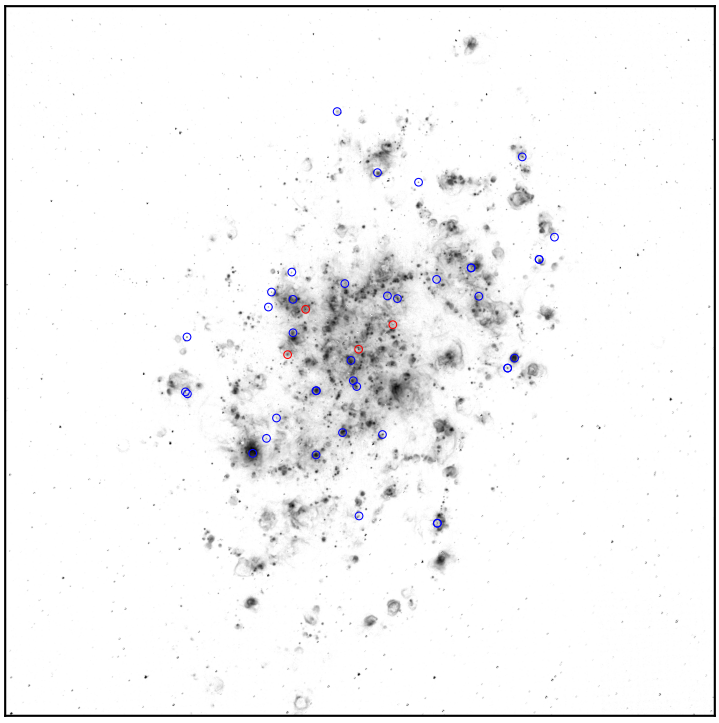

Figure 3.1: NCR processed image of M 33 without blurring or binning. The red circles show the locations of confirmed LBVs, and the blue show candidates. Note the resolved points in the centers of the circles, which is the stars themselves.

of the environment of the stars, rather than the strength of emission of the star itself, the images needed to be degraded to the point that the stars would be unresolved, and the pixels containing them would also contain their environment.

To achieve this, we degraded the images such that the resolution was equivalent to what it would be if each galaxy was 20 Mpc away and the images had an angular resolution of $1''$, following the procedure of Kangas et al. [48]. A Gaussian blur was applied to each image to achieve the degradation of resolution. The Gaussian blur applied to each image had a standard deviation equal to the desired FWHM for the degraded image divided by 2.355.[1]

[1]The standard deviation is divided by 2.355 because the FWHM of a Gaussian distribution is equal to 2.355 times the standard deviation of the distribution.

## 3.3 Processing of M 31

To create a continuum subtracted H $\alpha$ image of M 31, we used H$\alpha$ and R-band exposures across ten fields from the Local Group Galaxies Survey [58] and identified LBVs from several catalogs. The reference catalog for each star is listed in Table 4.1. We first aligned and multiplicatively scaled each individual field using AstroImageJ [16] such that stars in the R-band exposures were the same brightness and in the same pixel position as in the H$\alpha$ exposures. Then, the scaled R-band exposures were subtracted from the H$\alpha$ exposures using astropy. This process was done to ensure that only H$\alpha$ emissions were present in the H$\alpha$ filter, with the extra R-band light removed.

After continuum subtracting each field, we noted that the second field had prominent dithering lines. These lines were present in the original release of the data (though were not noticeable before continuum subtraction). Because the first and third fields overlap, we were able to omit the second field from our processing while maintaining full view of the galaxy.

After continuum subtracting the nine individual fields of M 31, we scaled the fields additively to each other.[2] The method we used was to let the first field be the baseline, and then scale the third field (since the second was excluded) such that the average values of the pixels where they overlapped were the same. This was repeated with the fourth field scaled to the third field, the fifth to the fourth, and so on for all the fields. Finally, we used the astropy reproject package [67] in Python to mosaic the nine fields together using the interpolation method of reprojection. After the mosaicing process was complete, a linear offset was applied to the entire image such that the average of the surrounding flux on the edges of the image was scattered around zero, as our background level.

For the degradation of M 31, we repeat our method from Section 3.2 to project the galaxy as 20 Mpc away, rather than its actual distance of 780 kpc [81]. A Gaussian blur with a standard deviation of 49.6 was applied using scipy [85] to increase the minimum FWHM of resolved stars from 4.5 pixels to 117 pixels to achieve this.

[2]This was the recommended method from private communication with Phil Massey, the first author of the data release for the original images.

After the blur was applied, the mosaiced galaxy image was binned by a factor of 26, such that each new pixel was made up of a block of 26 x 26 pixels from the original image. This corresponded to the image resolution if the exposures were taken of a galaxy 20 Mpc away.

In spite of the continuum subtraction, many noticeable foreground stars still remained. Due to these stars producing H$\alpha$ not actually in M 31, they were masked in order for the normalized cumulative ranking to be accurate.

## 3.4 Pixel Statistics

To rank how well the cLBVs and LBVs are associated with regions of ongoing SF, we found the normalized cumulative rank (NCR) for each cLBV and LBV. NCR is a ranking of the strength of signal of a pixel relative to the rest of the image, ranging from zero (background) to one (the brightest pixel in the image). This method was first described in James & Anderson [46]. Also see Anderson et al. [5], Habergham et al. [33], Kangas et al. [48], and Ransome et al. [69] for later uses of the method. To achieve this, we used python and the astropy package to first transformed the pixel values from each H$\alpha$ image into a 1D array. Then, we sorted the array in ascending order while storing the original pixel positions and cumulatively summed it. The cumulative sum for each pixel was then divided by the cumulative sum of the whole, and all negative values set to zero, giving an NCR value for each pixel ranging from zero to one. The array is then reordered such that each transformed (NCR) value is put back to its original position, giving an "intensity map" of the H$\alpha$ emission (and thus, SF regions) in each galaxy.

As mentioned in Section 3.1, certain regions of the continuum subtracted images had to be masked out. These regions were ignored in the cumulatively summing operation and then assigned a value of zero in the final step when the values are rearranged back into an image. One of the LBVs was found in a masked region (when there could have been H$\alpha$ present that was over-subtracted) and one was found outside the image itself, so they was removed from the dataset to avoid false assignment of "zero" NCR.

With the transformed images, we found the pixel value for each cLBV and LBV in its respective host galaxy. We did this by finding the pixels containing each cLBV and LBV using the astropy SkyCoord functions and assigning the stars the NCR of their respective pixels. With these NCR values, we can construct NCR distributions and perform statistical tests to to test the similarity between the NCR distributions of LBVs and cLBVs and other distributions.

For a population distribution that perfectly follows H$\alpha$, the sample would have a uniform NCR distribution. In this case, 70% of the sample would have an NCR $\leq 0.7$, or be coming from "less strong" pixels, as the bottom 70% of H$\alpha$ emitting pixels have an NCR $\leq 0.7$. The mean NCR of a uniform distribution would thus be 0.5.

## 3.5 Radial Analysis

We also performed radial analysis on suitable H$\alpha$ images of select galaxies . Radial analysis is a process that has been used for similar studies, such as Habergham et al. [33] and Ransome et al. [69], where it was used to essentially asses the radial offset of SNe from the center of the galaxy in terms of the light from a specific band. In our radial analysis, each LBV is given a value from 0 to 1 that ranks how close it is to the center of a galaxy in a given band. The value is given by first finding the ellipse for the galaxy that contains the extent of flux in a given band (in this case, H$\alpha$ and R). This is determined to be where the amount of flux added when increasing aperture size is within error of background levels of the image. Then, for each LBV, an ellipse with the same eccentricity and center is found that intersects the LBV. Each LBV then gets a value, Fr(H$\alpha$) or Fr(R), which is the amount of flux contained by the LBV's bisecting ellipse in a given band as a fraction of the total flux contained in the host in that band.

After performing radial analysis on the LBVs in our selected hosts, we also examined possible correlations between each LBV's NCR and Fr(R) values. This was done by finding the Pearson correlation coefficient [65] of NCR plotted against fraction of R-band flux. This process was repeated for the SNe IIn analyzed in Ransome et al. [69] for comparison.

## 3.6 Statistical tests

For our statistical analysis, we employed primarily the two-sample Anderson-Darling (AD) test and two-sample Wasserstein (WS) test. The AD test was used to compare empirical NCR distributions due to putting greater weight on the tails of distributions tested, which is an improvement over the two-sample Kolmogorov-Smirnov test for distributions where data points [4]. Additionally, the AD test has an overall greater statistical power, or an overall greater chance of correctly rejecting a null hypothesis [14], for comparing populations than the two-sample KS test [70]. The WS test was also used due to having more power than the AD test [34], but is uncommon in the field of astronomy. Therefore, the inclusion of the AD test allows more direct comparison of p-values to other works in the field, while the WS test is considered more versatile overall.

The tests were used to compare each data set against a hypothetical data set with perfectly uniform cumulative distribution (CD) (i.e. a uniform NCR distribution). To do this, we generated samples with the same number of data points as the real observations distributed such that their simulated NCRs perfectly aligned with a uniform cumulative distribution.

Additionally, the aforementioned two-sample tests were used to compare the LBV NCR sample against the SNe IIn sample collected by Ransome et al. [69]. Both the total sample and the non-zero NCR sample of SNe IIn were compared against in order to determine which sample LBVs could be most associated with as progenitors.

# Chapter 4

# Results

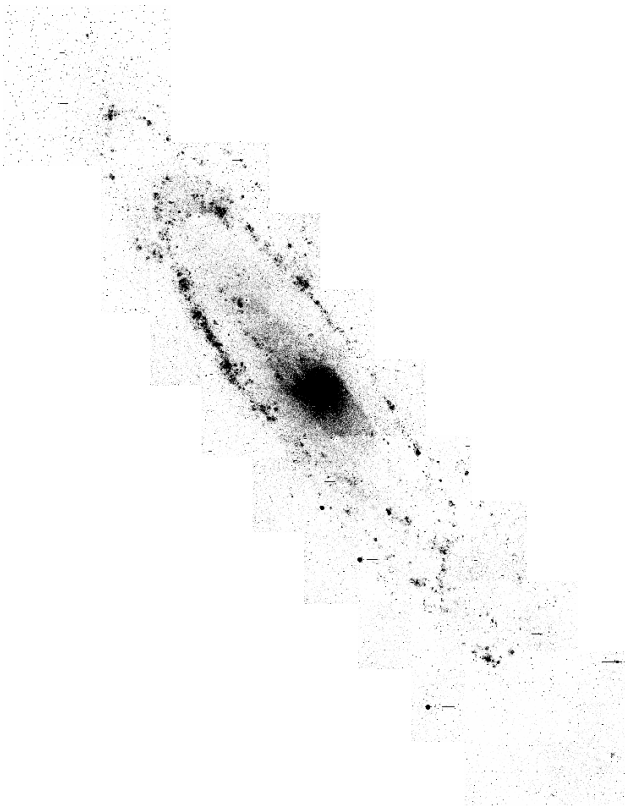

Figure 4.1: Compressed continuum-subtracted H$\alpha$ image of the full M 31 galaxy.

## 4.1 Continuum Reduced Image of M 31

One of our primary goals for this project was to produce a complete continuum subtracted H$\alpha$ image of M 31, which we accomplished. One field had to be removed entirely due to dithering present in the original image (see Section 3.3). However, due to how much the original fields overlap, the entirety of the galaxy itself is included in the final image, with only some background missing on one part of the edge of the galaxy. A compressed version of the image is shown in Figure 4.1, while the full size FITS file is available upon request.

## 4.2 NCR distribution of cLBVs and LBVs

The full results of our NCR analysis is shown in Table 4.1. We performed all statistical tests used for the total combined LBV sample (including both recognized LBVs and candidates), as

well as for only the sample of confirmed LBVs and the sample of candidate LBVs individually. However, an AD test and a WS test both suggest that the LBVs and cLBVs come from the same distribution, with p-values of 0.94 and 0.95, respectively. P-values describe the probability that a randomly generated distribution is as distinct (or more so) from the null result than the actual data is. A low p-value ($< 0.05$ is typical for most fields, such as astronomy) shows that a result is significant, but a p-value greater that that does not prove the negative. The results of comparing the NCR distributions LBVs to cLBVs with the AD and WS tests are consistent with Smith [76] in regards to the environments of LBVs compared to cLBVs.

The full sample had a median NCR of 0.46 and a mean NCR of $0.46 \pm 0.03$, using standard error of mean. This is consistent with the sample tracing H$\alpha$ emission, with the mean falling within two error bars of the hypothetical mean NCR of 0.50 of a population that perfectly followed H$\alpha$ emission. The median NCR of the confirmed population is 0.46, and the mean is $0.47 \pm 0.03$, while the candidate population has a median NCR of 0.46 and mean of $0.46 \pm 0.03$. The mean NCR of both the candidate population and the confirmed population are consistent with each other, as well as consistent with a uniform distribution.

The AD and WS tests of the combined sample versus a uniform distribution yield p-values of 0.12 and 0.30, respectively. This suggests the combined sample is statistically consistent with being drawn from the same parent distribution as a uniform distribution. These tests yield p-values of 0.60 and 0.82, respectively, for the confirmed population, and p-values of 0.18 and 0.34, respectively, for the candidate sample, suggesting they too are consistent with a uniform distribution.

Table 4.1: The IDs, host galaxies, spectral type, NCR, and fraction of flux associated with each star for H$\alpha$ and R bands for every star in our sample.

| Star ID | Host Galaxy | RA | Dec | Sp Type | NCR | Fr(H$\alpha$) | FR(R) | Reference |
|---|---|---|---|---|---|---|---|---|
| J013235.22+303017.5 | M 33 | 1h32m35.22s | 30d30m17.5s | cLBV | 0.189 | 0.94 | 0.92 | [59] |
| J013242.23+302114.0 | M 33 | 1h32m42.23s | 30d21m14.0s | cLBV | 0.421 | 0.96 | 0.94 | [59] |
| J013248.23+303950.3 | M 33 | 1h32m48.23s | 30d39m50.3s | cLBV | 0.101 | 0.87 | 0.85 | [59] |
| J013259.99+303332.3 | M 33 | 1h32m59.99s | 30d33m32.3s | cLBV | 0.525 | 0.73 | 0.69 | [59] |
| J013303.06+303101.7 | M 33 | 1h33m03.06s | 30d31m01.7s | cLBV | 0.495 | 0.71 | 0.68 | [59] |
| J013317.02+305329.8 | M 33 | 1h33m17.02s | 30d53m29.8s | cLBV | 0.447 | 0.90 | 0.88 | [59] |
| J013324.59+302328.3 | M 33 | 1h33m24.59s | 30d23m28.3s | cLBV | 0.000 | 0.78 | 0.74 | [59] |
| J013333.19+303343.3 | M 33 | 1h33m33.19s | 30d33m43.3s | cLBV | 0.583 | 0.26 | 0.29 | [59] |
| J013339.49+304540.4 | M 33 | 1h33m39.49s | 30d45m40.4s | cLBV | 0.518 | 0.37 | 0.38 | [59] |
| J013341.25+302237.1 | M 33 | 1h33m41.25s | 30d22m37.1s | cLBV | 0.188 | 0.80 | 0.77 | [59] |
| J013349.25+305250.1 | M 33 | 1h33m49.25s | 30d52m50.1s | cLBV | 0.275 | 0.69 | 0.66 | [59] |
| J013350.09+304126.5 | M 33 | 1h33m50.09s | 30d41m26.5s | cLBV | 0.732 | 0.04 | 0.05 | [59] |
| J013352.39+303909.5 | M 33 | 1h33m52.39s | 30d39m09.5s | cLBV | 0.876 | 0.01 | 0.01 | [59] |
| J013355.93+304530.5 | M 33 | 1h33m55.93s | 30d45m30.5s | cLBV | 0.885 | 0.19 | 0.24 | [59] |
| J013357.70+301714.1 | M 33 | 1h33m57.70s | 30d17m14.1s | cLBV | 0.204 | 0.98 | 0.96 | [59] |
| J013406.60+304147.7 | M 33 | 1h34m06.60s | 30d41m47.7s | cLBV | 0.769 | 0.13 | 0.17 | [59] |
| J013416.07+303344.8 | M 33 | 1h34m16.07s | 30d33m44.8s | cLBV | 0.715 | 0.49 | 0.54 | [59] |
| J013416.41+303120.7 | M 33 | 1h34m16.41s | 30d31m20.7s | cLBV | 0.070 | 0.67 | 0.64 | [59] |
| J013422.88+304410.9 | M 33 | 1h34m22.88s | 30d44m10.9s | cLBV | 0.190 | 0.42 | 0.44 | [59] |
| J013424.75+303306.5 | M 33 | 1h34m24.75s | 30d33m06.5s | cLBV | 0.116 | 0.71 | 0.67 | [59] |
| J013426.08+303424.6 | M 33 | 1h34m26.08s | 30d34m24.6s | cLBV | 0.000 | 0.68 | 0.65 | [59] |
| J013459.44+303701.8 | M 33 | 1h34m59.44s | 30d37m01.8s | cLBV | 0.000 | 0.94 | 0.92 | [59] |
| J013500.27+304150.8 | M 33 | 1h35m00.27s | 30d41m50.8s | cLBV | 0.340 | 0.91 | 0.88 | [59] |
| J013335.11+303600.3 | M 33 | 1h33m35.11s | 30d36m00.3s | LBV | 0.459 | 0.15 | 0.19 | [59] |
| J013349.20+303809.0 | M 33 | 1h33m49.20s | 30d38m09.0s | LBV | 0.669 | 0.02 | 0.03 | [59] |
| J013410.90+303437.5 | M 33 | 1h34m10.90s | 30d34m37.5s | LBV | 0.629 | 0.42 | 0.44 | [59] |
| J013418.36+303836.9 | M 33 | 1h34m18.36s | 30d38m36.9s | LBV | 0.456 | 0.40 | 0.41 | [43] |
| J013229.00+302819.5 | M 33 | 1h32m29.00s | 30d28m19.5s | cLBV | 0.246 | 0.98 | 0.96 | [43] |

| Star ID | Host Galaxy | RA | Dec | Sp Type | NCR | Fr(H$\alpha$) | FR(R) | Reference |
|---|---|---|---|---|---|---|---|---|
| J013235.22+303017.5 | M 33 | 1h32m35.22s | 30d30m17.5s | cLBV | 0.189 | 0.94 | 0.92 | [43] |
| J013245.38+303858.2 | M 33 | 1h32m45.38s | 30d38m58.2s | cLBV | 0.935 | 0.89 | 0.87 | [43] |
| J013248.23+303950.3 | M 33 | 1h32m48.23s | 30d39m50.3s | cLBV | 0.101 | 0.87 | 0.85 | [43] |
| J013303.10+303101.9 | M 33 | 1h33m03.10s | 30d31m01.9s | cLBV | 0.495 | 0.71 | 0.68 | [43] |
| J013317.02+305329.8 | M 33 | 1h33m17.02s | 30d53m29.8s | cLBV | 0.447 | 0.90 | 0.88 | [43] |
| J013317.19+303201.5 | M 33 | 1h33m17.19s | 30d32m01.5s | cLBV | 0.267 | 0.46 | 0.51 | [43] |
| J013337.32+303328.9 | M 33 | 1h33m37.32s | 30d33m28.9s | cLBV | 0.410 | 0.23 | 0.27 | [43] |
| J013351.43+304056.9 | M 33 | 1h33m51.43s | 30d40m56.9s | cLBV | 0.801 | 0.02 | 0.03 | [43] |
| J013354.82+303222.7 | M 33 | 1h33m54.82s | 30d32m22.7s | cLBV | 0.433 | 0.36 | 0.37 | [43] |
| J013406.63+304147.7 | M 33 | 1h34m06.63s | 30d41m47.7s | cLBV | 0.769 | 0.13 | 0.17 | [43] |
| J013406.77+304726.9 | M 33 | 1h34m06.77s | 30d47m26.9s | cLBV | 0.903 | 0.35 | 0.36 | [43] |
| J013416.04+303642.0 | M 33 | 1h34m16.04s | 30d36m42.0s | cLBV | 0.484 | 0.42 | 0.43 | [43] |
| J013427.08+304559.7 | M 33 | 1h34m27.08s | 30d45m59.7s | cLBV | 0.130 | 0.47 | 0.51 | [43] |
| J013432.73+304717.1 | M 33 | 1h34m32.73s | 30d47m17.1s | cLBV | 0.000 | 0.60 | 0.60 | [43] |
| J013459.36+304201.1 | M 33 | 1h34m59.36s | 30d42m01.1s | cLBV | 0.369 | 0.90 | 0.88 | [43] |
| J003910.85+403622.4 | M 31 | 0h39m10.85s | 40d36m22.4s | cLBV | 0.393 | — | — | [59] |
| J004051.59+403303.0 | M 31 | 0h40m51.59s | 40d33m03.0s | cLBV | 0.553 | — | — | [56] |
| J004109.11+404853.2 | M 31 | 0h41m09.11s | 40d48m53.2s | cLBV | 0.631 | — | — | [59] |
| J004221.78+410013.4 | M 31 | 0h42m21.78s | 41d00m13.4s | cLBV | 0.423 | — | — | [63] |
| J004229.87+410551.8 | M 31 | 0h42m29.87s | 41d05m51.8s | cLBV | 0.467 | — | — | [58] |
| J004302.52+414912.4 | M 31 | 0h43m02.52s | 41d49m12.4s | LBV | 0.290 | — | — | [73][40] |
| J004320.97+414039.6 | M 31 | 0h43m20.97s | 41d40m39.6s | cLBV | 0.458 | — | — | [52] |
| J004322.50+413940.9 | M 31 | 0h43m22.50s | 41d39m40.9s | cLBV | 0.280 | — | — | [58] |
| J004333.09+411210.4 | M 31 | 0h43m33.09s | 41d12m10.4s | LBV | 0.712 | — | — | [39][40] |
| J004341.84+411112.0 | M 31 | 0h43m41.84s | 41d11m12.0s | cLBV | 0.743 | — | — | [55] |
| J004350.50+414611.4 | M 31 | 0h43m50.50s | 41d46m11.4s | cLBV | 0.196 | — | — | [58] |
| J004411.36+413257.2 | M 31 | 0h44m11.36s | 41d32m57.2s | cLBV | 0.708 | — | — | [52] |
| J004415.00+420156.2 | M 31 | 0h44m15.00s | 42d01m56.2s | cLBV | 0.000 | — | — | [58] |
| J004417.10+411928.0 | M 31 | 0h44m17.10s | 41d19m28.0s | cLBV | 0.656 | — | — | [52] |
| J004419.43+412247.0 | M 31 | 0h44m19.43s | 41d22m47.0s | LBV | 0.378 | — | — | [39][40] |
| J004425.18+413452.2 | M 31 | 0h44m25.18s | 41d34m52.2s | cLBV | 0.606 | — | — | [52] |

| Star ID | Host Galaxy | RA | Dec | Sp Type | NCR | Fr(H$\alpha$) | FR(R) | Reference |
|---|---|---|---|---|---|---|---|---|
| J004442.28+415823.1 | M 31 | 0h44m42.28s | 41d58m23.1s | cLBV | 0.629 | — | — | [58] |
| J004444.01+415152.0 | M 31 | 0h44m44.01s | 41d51m52.0s | cLBV | 0.399 | — | — | [59] |
| J004444.52+412804.0 | M 31 | 0h44m44.52s | 41d28m04.0s | cLBV | 0.872 | — | — | [58] |
| J004450.54+413037.7 | M 31 | 0h44m50.54s | 41d30m37.7s | LBV | 0.719 | — | — | [39][40] |
| J004507.65+413740.8 | M 31 | 0h45m07.65s | 41d37m40.8s | cLBV | 0.773 | — | — | [58] |
| J004522.58+415034.8 | M 31 | 0h45m22.58s | 41d50m34.8s | cLBV | 0.622 | — | — | [58] |
| J004526.62+415006.3 | M 31 | 0h45m26.62s | 41d50m06.3s | cLBV | 0.749 | — | — | [58] |
| J004621.08+421308.2 | M 31 | 0h46m21.08s | 42d13m08.2s | cLBV | 0.000 | — | — | [52] |
| NGC 4736_1 | NGC 4736 | 12h50m57.60s | 41d07m23.1s | LBV | 0.035 | — | — | [79] |
| SN 2005gl | NGC 266 | 0h49m50.02s | 32d16m56.8s | LBV | 0.313 | — | — | [25] |
| TS V37 | NGC 2403 | 7h37m01.83s | 65d34m29.3s | LBV | 0.000 | — | — | [44] |
| EV* N2403 V0038 | NGC 2403 | 7h37m10.23s | 65d33m11.2s | LBV | 0.000 | — | — | [44] |
| J002012.10+591848.0 | IC 10 | 0h20m12.10s | 59d18m48.0s | cLBV | 0.342 | — | — | [58] |
| J002016.40+591906.9 | IC 10 | 0h20m16.40s | 59d19m06.9s | cLBV | 0.458 | — | — | [58] |
| J002020.30+591837.6 | IC 10 | 0h20m20.30s | 59d18m37.6s | cLBV | 0.416 | — | — | [58] |
| V* S Dor | LMC | 5h18m14.36s | -69d15m01.1s | LBV | 0.725 | 0.10 | 0.06 | [1] |
| HD 269858 | LMC | 5h36m43.69s | -69d29m47.5s | LBV | 0.797 | 0.22 | 0.24 | [1] |
| CPD-69 463 | LMC | 5h38m51.62s | -69d08m07.3s | LBV | 0.979 | 0.31 | 0.34 | [1] |
| HD 269662 | LMC | 5h30m51.47s | -69d02m58.6s | LBV | 0.579 | 0.16 | 0.14 | [1] |
| HD 269321 | LMC | 5h17m56.07s | -69d16m03.8s | cLBV | 0.725 | 0.10 | 0.06 | [1] |
| LHA 120-S 61 | LMC | 5h45m51.94s | -67d14m25.9s | cLBV | 0.341 | 0.77 | 0.85 | [1] |
| HD 269687 | LMC | 5h31m25.52s | -69d05m38.6s | cLBV | 0.579 | 0.16 | 0.14 | [1] |
| HD 269582 | LMC | 5h27m52.66s | -68d59m08.5s | LBV | 0.474 | 0.14 | 0.10 | [1] |
| SK -69 279 | LMC | 5h41m44.66s | -69d35m14.9s | cLBV | 0.589 | 0.35 | 0.38 | [1] |
| HD 269128 | LMC | 5h10m22.79s | -68d46m23.8s | cLBV | 0.334 | 0.33 | 0.36 | [1] |
| HD 269227 | LMC | 5h13m54.28s | -69d31m46.7s | cLBV | 0.326 | 0.14 | 0.11 | [1] |
| HD 269445 | LMC | 5h22m59.79s | -68d01m46.6s | cLBV | 0.473 | 0.39 | 0.44 | [1] |
| HD 37974 | LMC | 5h36m25.85s | -69d22m55.8s | cLBV | 0.840 | 0.23 | 0.24 | [1] |
| CPD-69 500 | LMC | 5h41m20.13s | -69d36m23.0s | cLBV | 0.589 | 0.33 | 0.37 | [1] |
| HD 268835 | LMC | 4h56m47.08s | -69d50m24.8s | cLBV | 0.000 | 0.56 | 0.63 | [1] |
| HD 268939 | LMC | 5h04m14.91s | -67d15m05.3s | cLBV | 0.144 | 0.74 | 0.83 | [1] |

| Star ID | Host Galaxy | RA | Dec | Sp Type | NCR | Fr(H$\alpha$) | FR(R) | Reference |
|---|---|---|---|---|---|---|---|---|
| LHA 120-S 18 | LMC | 5h05m53.98s | -68d10m50.5s | cLBV | 0.128 | 0.53 | 0.60 | [1] |
| HD 269050 | LMC | 5h07m20.42s | -68d32m08.6s | cLBV | 0.237 | 0.44 | 0.51 | [1] |
| HD 269216 | LMC | 5h13m30.78s | -69d32m23.6s | LBV | 0.326 | 0.15 | 0.12 | [1] |
| HD 34664 | LMC | 5h13m52.99s | -67d26m54.8s | cLBV | 0.510 | 0.60 | 0.68 | [1] |
| HD 269604 | LMC | 5h28m31.37s | -68d53m55.7s | cLBV | 0.411 | 0.17 | 0.14 | [1] |
| HD 269700 | LMC | 5h31m52.28s | -68d32m38.9s | cLBV | 0.650 | 0.30 | 0.32 | [1] |
| HD 37836 | LMC | 5h35m16.63s | -69d40m38.4s | cLBV | 0.845 | 0.18 | 0.17 | [1] |
| HD 269859 | LMC | 5h36m47.19s | -69d29m52.1s | cLBV | 0.797 | 0.23 | 0.24 | [1] |
| RMC 149 | LMC | 5h39m58.74s | -69d44m04.1s | cLBV | 0.691 | 0.30 | 0.32 | [1] |
| HD 38489 | LMC | 5h40m13.32s | -69d22m46.5s | cLBV | 0.655 | 0.32 | 0.35 | [1] |
| EM* MWC 112 | LMC | 5h28m21.97s | -68d59m48.3s | LBV | 0.432 | 0.14 | 0.10 | [1] |
| HD 269006 | LMC | 5h02m07.39s | -71d20m13.1s | LBV | 0.000 | 0.58 | 0.65 | [78] |
| SK -69 279 | LMC | 5h41m44.66s | -69d35m14.9s | LBV | 0.589 | 0.35 | 0.38 | [78] |
| HD 5980 | SMC | 0h59m26.58s | -72d09m53.9s | LBV | 0.934 | 0.30 | 0.63 | [78] |
| HD 6884 | SMC | 1h07m18.22s | -72d28m03.7s | LBV | 0.219 | 0.44 | 0.86 | [78] |
| LHA 115-S 6 | SMC | 0h46m55.03s | -73d08m34.1s | cLBV | 0.920 | 0.16 | 0.32 | [82] |
| LHA 115-S 18 | SMC | 0h54m09.54s | -72d41m43.3s | cLBV | 0.579 | 0.02 | 0.05 | [83] |

In addition to the statistical tests performed, we also mapped the LBVs and cLBVs onto transformed images of their host galaxies. The pixel values for the images are simply the NCR values of each pixel, on a grey-scale of 0 to 1 (0 being white, 1 being black). These are shown in Figures 4.2 (a) and (b), 4.3 (a) and (b), and 4.4 (a) and (b). The circles show the location of cLBVs in cyan and confirmed LBVs in red. The circle size is the same angular diameter in all images except in NGC 266, which was not binned due to already being so distant (64.01 $\pm$ 4.49 Mpc, which is even further than we distort to [80]) and low spatial resolution.

## 4.3 NCR distribution of LBVs compared to SNe IIn

As one of the primary motivations for this study was investigating LBVs as progenitors of SNe IIn, we performed a variety of tests comparing the LBVs sampled to the SNe IIn sample studied in Ransome et al. [69]. For these population comparisons, we used an AD test and a WS test.

An AD test between the combined LBV sample and the total SNe IIn sample gives a p-value $\leq 0.001$, suggesting with a high degree of confidence that the combined LBV sample and the total SNe IIn sample do not share the same parent distributions. The sample of candidates against the SNe IIn also have a p-value $\leq 0.001$, while the sample of confirmed LBVs have a p-value of 0.013, both being above the 95% confidence interval for being taken from separate populations. The WS test also yields p-values $\leq 0.001$ for the combined and candidate samples, and a p-value of 0.035 for the confirmed sample. This supports the AD test in suggesting both candidate population and the the confirmed population have different parent population distributions from the total population of SNe IIn.

Ransome et al. [69] noted that non-zero NCR SNe IIn do trace H$\alpha$ emission well, suggesting multiple progenitor populations for the SN type. Therefore, we performed goodness-of-fit tests against the non-zero NCR SN IIn population as well.

An AD test and WS yield p-values of 0.019 and 0.088, respectively, for the combined set, and 0.022 and 0.091, respectively, for the candidate set compared to the non-zero NCR SN IIn set. The

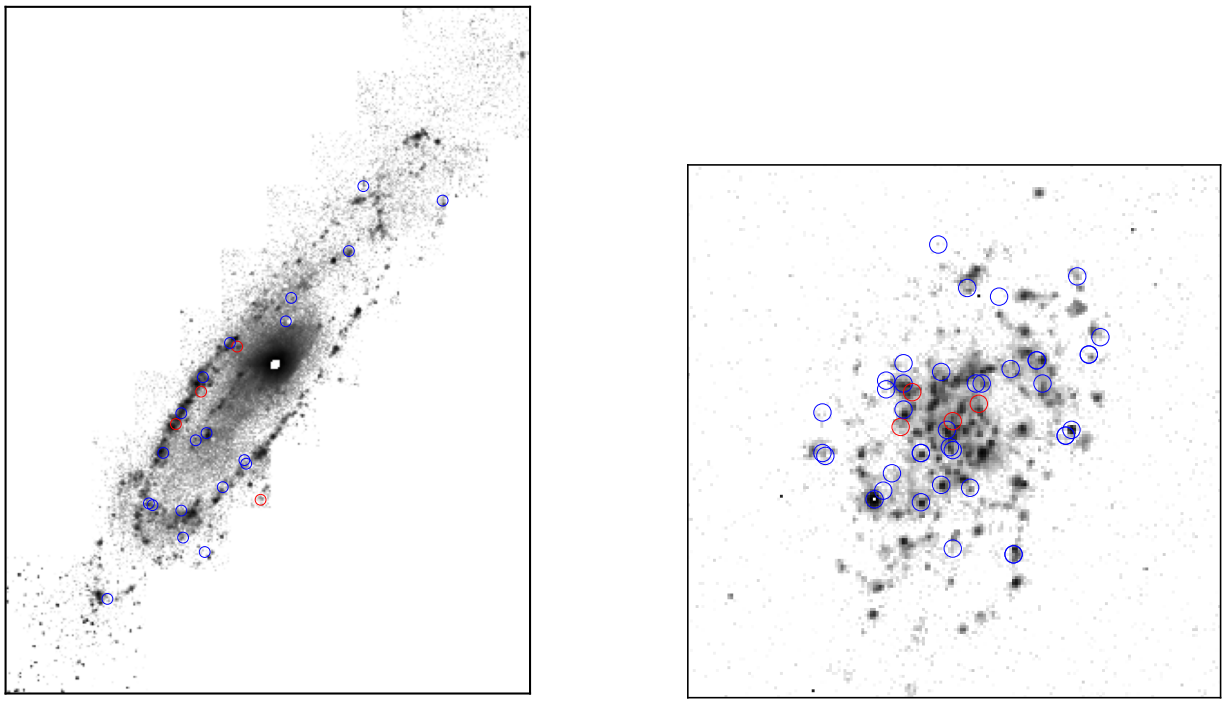

(a) M 31

(b) M 33

Figure 4.2: LBVs and cLBVs spatially plotted onto the NCR images of M 31 and the M 33. Confirmed LBVs are shown by red circles, and candidates are cyan.

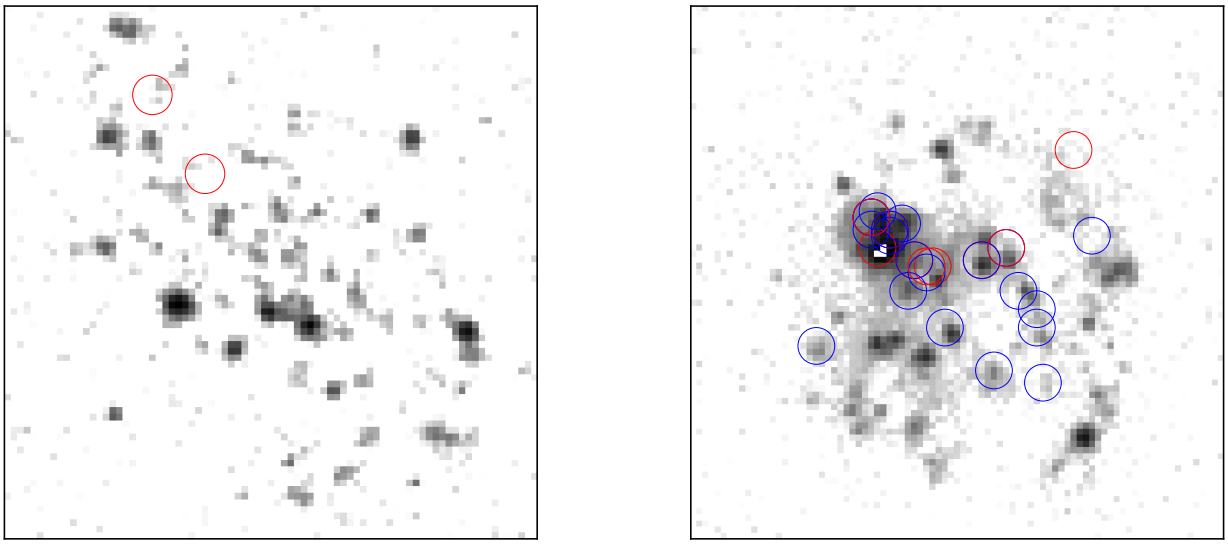

(a) NGC 2403

(b) LMC

Figure 4.3: LBVs and cLBVs spatially plotted onto the NCR images of NGC 2403 and the LMC. Confirmed LBVs are shown by red circles, and candidates are cyan.

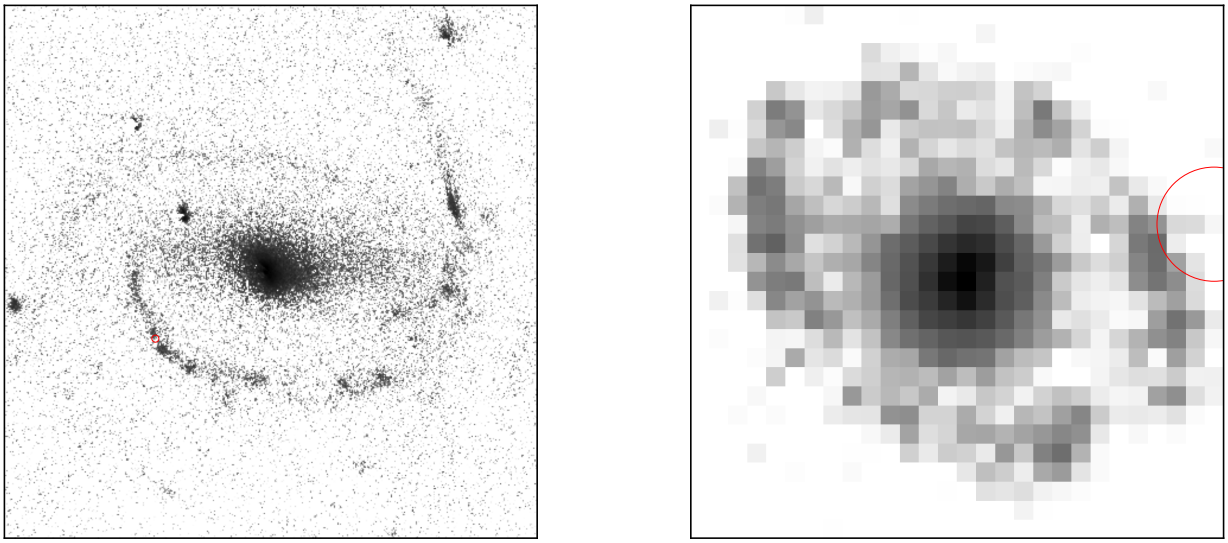

(a) NGC 266

(b) NGC 4736

Figure 4.4: LBVs plotted onto the NCR images of NGC 266 and NGC 4736. NGC 266's LBV is actually the location of SN 2005gl, which had an LBV progenitor. Both LBVs are confirmed, and thus plotted in red.

AD test suggests the combined and candidate samples are inconsistent with coming from the same parent distribution as the non-zero NCR SNe IIn, while the WS test suggests they are consistent if using a p-value of $\leq 0.05$ as significant for being drawn from a distinct population.

For the confirmed sample compared to the non-zero NCR SNe IIn, the AD test and the WS test yield p-values of 0.16 and 0.32, respectively. These both suggest that the confirmed LBV sample is consistent with coming from the same parent distribution as the non-zero NCR SN IIn sample. This is in contrast to the AD test results for the combined and candidate samples. While the p-value of 0.32 for the WS test of the confirmed sample compared to the non-zero NCR SNe IIn is higher than those for the combined and candidates samples (with p-values of 0.088 and 0.091), all three sets are statistically consistent with being drawn from the same parent distribution as the non-zero NCR SNe IIn sample using the WS test and a p-value of $\leq 0.05$ as significant for being drawn from a distinct population. That being said,

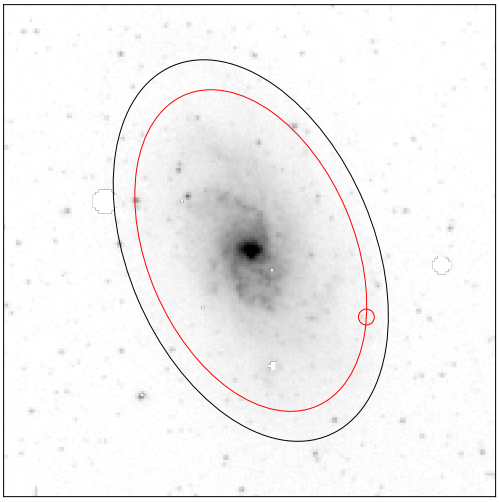

Figure 4.5: Radial analysis visualization of M 33 in the R-band. The red ellipse intersects the cLBV J013235.22+303017.5, and contains 92% of the R-band flux of the galaxy.

## 4.4 Radial Analysis of Hosts

Figure 4.5 shows an example of radial analysis in M 33. The figure shows the black ellipse containing all of the R-band flux of M 33, while the red ellipse intersects the cLBV J013235.22+303017.5. The ellipse intersecting J013235.22+303017.5 contains 92% of the total R-band flux contained in the galaxy's ellipse, so J013235.22+303017.5 has an"Fr(R)" value of 0.92. Table 4.1 also shows the results of our radial analysis for all LBVs and cLBVs in hosts where radial analysis was possible.

The Pearson correlation coefficient for the combined sample's NCR versus R-band flux fraction was found to be -0.58 $\pm$ 0.07 with a p-value $\leq$ 0.01. For the confirmed sampled it was found to be -0.3 $\pm$ 0.3 with a p-value of 0.34, and the candidate sample had test statistic of -0.62 $\pm$ 0.08 and a p-value $\leq$ 0.01. The non-zero SNe IIn sample's NCR versus R-band flux fraction yielded a test statistic of -0.57 $\pm$ 0.14 and a p-value $\leq$ 0.01. The Pearson correlation coefficients suggest that the NCR values of the combined and candidate LBV samples and the non-zero SNe IIn are negatively correlated with R-band flux fraction, while the coefficient for the purely confirmed LBV sample

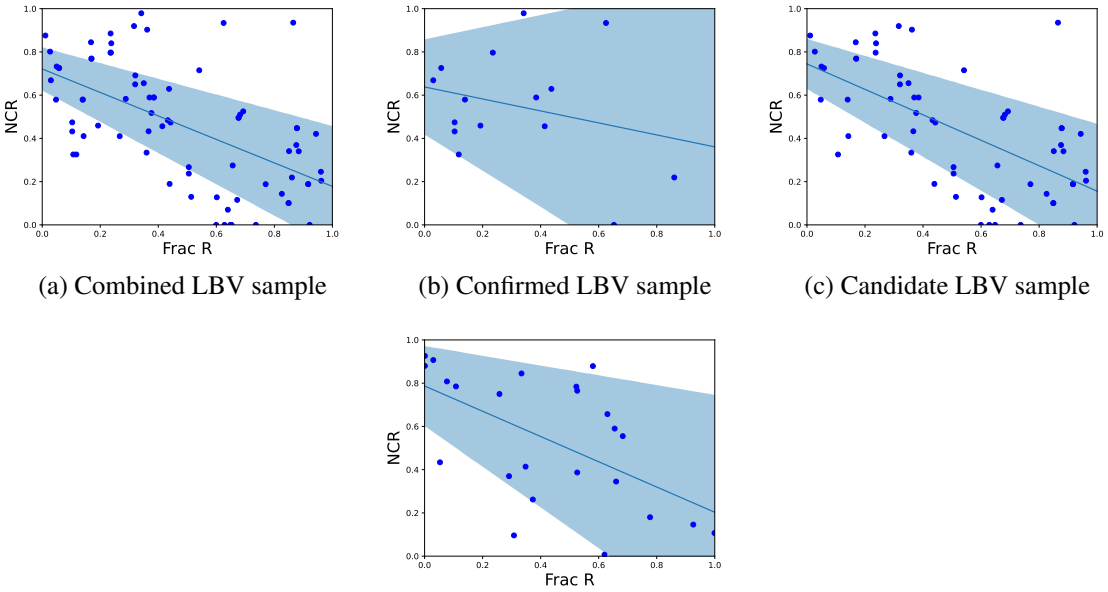


(a) Combined LBV sample (b) Confirmed LBV sample (c) Candidate LBV sample

(d) SNe IIn sample [69]

Figure 4.6: Radial distribution in the R-band (as fraction of contained flux) vs NCR for the combined sample of LBVs, the confirmed sample of LBVs, the candidate sample, and the non-zero NCR SNe IIn from Ransome et al. [69].

suggests there is no significant correlation for the set. These results are plotted in Figures 4.6 (a), (b), (c), and (d). The shaded area represents a 95% confidence interval for the trendlines.

Additionally, we performed AD and WS tests comparing the different samples' R-band distribution as Fr(R). The AD and WS tests comparing the combined sample with the non-zero NCR SNe IIn yielded p-values of 0.59 and 0.60, respectively. For the confirmed sample and the non-zero NCR SNe, the p-values were 0.34 and 0.22, respectively, and they were 0.28 for both tests for the candidates and the non-zero SNe IIn. All tests suggests all sets of LBV samples are consistent with being drawn from the same underlying radial distribution in the R-band as non-zero NCR SNe IIn.

We also compared the radial distribution between the candidate and the confirmed samples. The p-values for the AD and WS tests between the candidate and confirmed LBV samples' R-band distribution were 0.019 and 0.017, respectively. This suggests that the candidate and confirmed samples have distinct radial R-band distributions with a 95% confidence interval. These results (along with the results for all other statistical tests) are summarized in Table 4.2.

Table 4.2: Summary of the results from our statistical tests.

| Comparison of NCR Distributions | | | | | | |
|---|---|---|---|---|---|---|
| | Combined LBVs | | Confirmed LBVs | | Candidate LBVs | |
| | AD Test | WS Test | AD Test | WS Test | AD Test | WS Test |
| Uniform Distribution | 0.12 | 0.30 | 0.60 | 0.82 | 0.18 | 0.34 |
| SNe IIn | $\leq 0.001$ | $\leq 0.001$ | 0.013 | 0.035 | $\leq 0.001$ | $\leq 0.001$ |
| Non-zero NCR SNe IIn | 0.019 | 0.088 | 0.16 | 0.32 | 0.022 | 0.091 |
| Candidate LBVs | — | — | 0.94 | 0.95 | — | — |

| Fr(R) vs NCR Pearson Coefficients | | | | |
|---|---|---|---|---|
| | Combined LBVs | Confirmed LBVs | Candidate LBVs | Non-zero NCR SNe IIn |
| Pearson Coefficient | -0.58 $\leq$ 0.07 | -0.3 $\leq$ 0.3 | -0.62 $\leq$ 0.08 | -0.57 $\leq$ 0.14 |
| P-Value | $\leq$ 0.01 | 0.34 | $\leq$ 0.01 | $\leq$ 0.01 |

| Comparison of Fr(R) Distributions | | | | | | |
|---|---|---|---|---|---|---|
| | Combined LBVs | | Confirmed LBVs | | Candidate LBVs | |
| | AD Test | WS Test | AD Test | WS Test | AD Test | WS Test |
| Non-zero NCR SNe IIn | 0.59 | 0.60 | 0.32 | 0.22 | 0.28 | 0.28 |
| Candidate LBVs | — | — | 0.019 | 0.017 | — | — |

# Chapter 5

# Discussion

Using LBVs and cLBVs from a total of eight different galaxies, we have performed the largest investigation of the environments of extragalactic LBVs and cLBVs to date. We investigated a sample of 23 confirmed LBVs and 84 candidates, measuring the association of the spectral type with ongoing SF as H$\alpha$ emission.

## 5.1 The environments of LBVs

Our analysis of the total LBV sample with the AD and WS tests suggests that their NCR distribution is consistent with a uniform distribution, and thus is consistent with it tracing regions of ongoing SF well. Additionally, the sample of only confirmed LBVs and only candidate LBVs are both consistent with a uniform distribution using the AD and WS tests as well. This uniform underlying NCR distribution of LBVs is consistent with Kangas et al. [48], which also found that LBVs are well-associated with regions of ongoing SF. It is also consistent with the notion of LBVs as young, very massive stars, and presents no surprises for what is known about them.

This result is consistent with a few possible evolutionary paths for LBVs and candidate LBVs (see Section 5.2). Although this method of analysis cannot provide precise ages for the sample investigated, it provides a lower bound (or lack thereof) on how young the stars are expected to be. Regions of high H$\alpha$ emission are characterized by their presence of young ($<$ 16 Myr [35]), massive ( $>$ 10 $M_{\odot}$) stars, the population of young stars within a galaxy is expected to trace this emission [49]. Although older stars could be in these regions as well, the sample showing only three LBVs outside of detectable emission, massive stars suggests the group as a whole is found almost exclusively in these regions, and is thus likely also made up of young, massive stars.

## 5.2 The evolution of LBVs

When considering the "traditional" evolutionary model of LBVs summarized in Humphreys & Davidson [41], our data for the confirmed LBV sample are consistent with evolving from massive stars. The timescale suggested in this model is well within the age limit we found for our

confirmed sample ($<$ 16 Myr). This timescale is consistent with the traditional, short-lived, single star evolution as discussed in Humphreys & Davidson [41], as well as the (relatively) longer lived binary evolution discussed in Smith & Tombleson [78], which still have lifespans $<$ 16 Myr. Given the broadness of what the pixel statistics method tells us about age, a different method would be needed to determine an age range more precise than just "young", such as taking spectra of the environments of the LBVs.

Similarly, our age bounds for the HII clouds can neither support nor reject the binary evolution models proposed by Smith & Tombleson [78] and Aghakhanloo et al. [3]. As mentioned before, while a binary model would allow LBV lifespans considerably longer than those of a single-star evolution, they would still fall within the $<$ 16 Myr upper bound we found for LBV ages due to the high masses of both binary stars. Even if the binary mechanism had two relatively "smaller" stars merging into the more massive LBV, both their masses ($>$ 10 $M_{\odot}$) are large enough for them to be short-lived stars. Once again, a more precise dating method would be needed as a followup to determine the validity of the timescale of such a model.

Additionally, the scale of distances in our images does not allow a precise follow-up to the study of LBV isolation in Smith & Tombleson [78] with a large sample using this method due to the hosts used being too distant. In most of the images used, each pixel was on the order of 10-100 pc in width (depending on the image) even before the degradation process, making precise distance measurements between LBVs and nearby O-type stars for the majority of our sample not possible. In the context of this study, even the smallest and oldest O-type stars contribute to the H$\alpha$ emission, so an LBV being well within an H$\alpha$ region could still be isolated from the largest O-type stars, as found in Smith & Tombleson [78]. Additionally, due to the scale issue, our data from the confirmed sample also can offer no answers on the validity of LBVs getting "kicked" away from an H$\alpha$-rich birthplace by super massive binary companions going SN.

## 5.3 Radial analysis of LBVs

From our radial analysis, one of the most significant findings was the distinctness of confirmed LBVs and candidate LBVs in their radial distribution in the R-band (see Section 5.5). The radial distribution in the R-band of the combined, confirmed, and candidate sets were all found to be consistent with sharing the same parent distribution function as the non-zero NCR SNe IIn, which is consistent with the NCR distributions in suggesting that the confirmed LBVs and non-zero NCR SNe IIn are drawn from the same population.

The finding of this correlation in the candidate and non-zero SNe IIn samples could have a variety of implications, and should be considered to be investigated further in a future study. As of now, it is unclear whether the R-band radial distribution - NCR relation is a property of the candidates and non-zero SNe IIn, or if it is a property of overall NCR distribution compared to R-band radial distribution. Additionally, Anderson et al. [5] found no correlation between Fr(R) vs NCR in the distribution of SNe II and SNe Ibc, so this could be a relation unique to LBVs and non-zero NCR SNe IIn (or perhaps any group of non-zero NCR stellar objects). This can be explored in future studies by doing the same R-band radial distribution vs NCR tests on other massive stars, such as red supergiants.

We also found significant correlation between radial distribution in the R-band (as fraction of contained flux) and NCR for the combined and candidate LBV samples, as well as in the non-zero SNe IIn from Ransome et al. [69]. The confirmed LBV sample did not display significant correlation, though the sample of confirmed LBVs able to be used for radial analysis was significantly smaller than what were able to be used for NCR analysis. The combined sample's found correlation is likely due solely to the distribution of candidates, whose greater number (compared to the confirmed sample) could be causing them to dominate the combined sample's distribution function.

The confirmed LBV sample's lack of a significant correlation between R-band radial distribution and NCR is notable in light of the correlation that was found in the cLBV sample and the

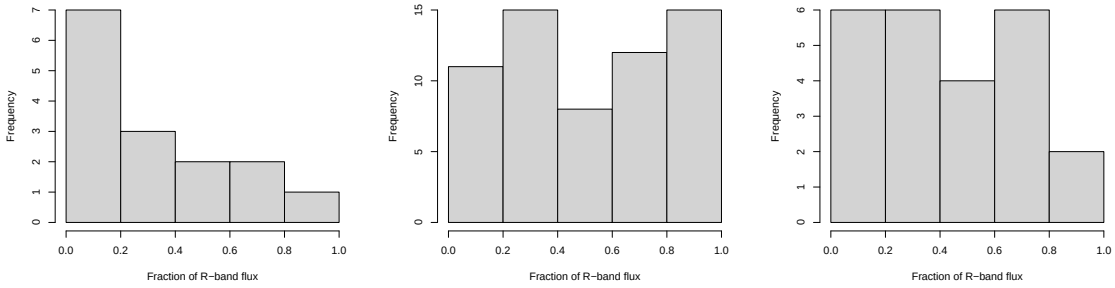


(a) Confirmed LBV sample (b) Candidate LBV sample (c) Non-zero NCR SNe IIn sample

Figure 5.1: Histograms of radial distribution in the R-band (as fraction of contained flux) for the the confirmed sample of LBVs, the candidate sample, and the non-zero NCR SNe IIn from Ransome et al. [69].

non-zero NCR SNe IIn sample, especially given the evidence that suggests confirmed LBVs may make up a portion of the progenitors of non-zero NCR SNe IIn. One possible explanation is that the lack of a found correlation might be due merely to the lack of confirmed LBVs found on the edge of the galaxy in the R-band (signified by a high fraction of contained flux). The sharp falloff as the contained flux fraction increases of the confirmed sample in comparison the the candidate sample and non-zero NCR SNe IIn sample can be seen in Figures 5.1a, 5.1b, and 5.1c.

## 5.4 LBVs as the progenitors of SNe IIn

When comparing the distributions of our confirmed sample, candidate sample, and the combined sample to the distribution of the total SN IIn sample surveyed in Ransome et al. [69], we find the samples are statistically inconsistent with coming from the same underlying distribution using the AD test and WS test. This result is expected, since Ransome et al. [69] found that the total SNe IIn sample had poor association with regions of ongoing SF. This finding is consistent with the findings of Kangas et al. [48], which also found LBVs to be inconsistent with their total sample of SNe IIn.

Comparing the non-zero NCR SNe IIn sample to the the confirmed sample as well as the combined sample LBVs with AD and WS tests shows that they are statistically consistent with

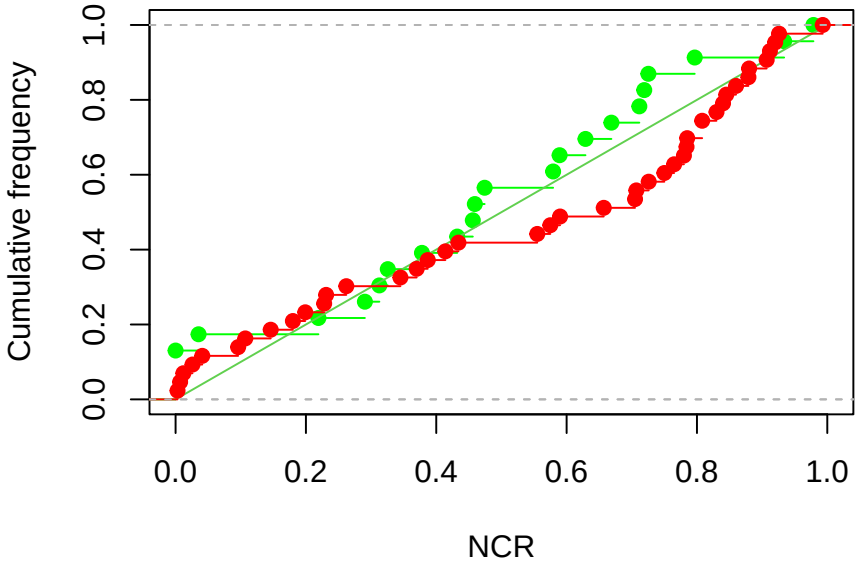


Figure 5.2: The empirical cumulative distribution of the confirmed LBV sample (green) and the non-zero NCR SNe IIn sample (red), plotted against a 1:1 NCR distribution.

being drawn from the same underlying distribution. The p-values for the AD and WS tests are both well within the bounds for both samples coming from the same distribution. These results suggest that LBVs may be a significant progenitor for SNe IIn that occur in regions of ongoing SF. While LBVs have been confirmed as one type of progenitor of SNe IIn since the observation of SN 2005gl's progenitor [25], this is the first study to quantitatively link the distributions of confirmed LBVs to the distribution of SNe IIn that are found in regions of ongoing SF. As these non-zero NCR SNe makes up over half of the known population of SNe IIn [69], this is a significant step toward confirming LBVs to be a significant progenitor of SNe IIn.

The sample of candidate LBVs, though, is statistically inconsistent with both the total and non-zero NCR sets of SNe IIn in both tests used. We suggest this is due to overall differences in the candidate and confirmed sample and candidates possibly including many stars that are not and will not become LBVs, as discussed in Section 5.5. Another possibility is that the LBV population truly is inconsistent with the distribution of non-zero NCR SNe IIn, and the apparent consistence of the confirmed sample is due to sampling size. While this seems unlikely due to the high p-values of the statistical tests comparing the distribution of confirmed LBVs and non-zero NCR SNe IIn, it is still a possibility. In this case, where the combined sample would be more statistically valid for comparison than the sample of confirmed LBVs, our data suggest that LBVs are progenitors of some, but not all, of the nonzero SNe IIn population. This would not be unprecedented, as although there has been a confirmed LBV progenitor to a SN IIn in SN 2005gl, Ransome et al. [69] found evidence of multimodality amongst the non-zero NCR SN IIn population. Thus, even if LBVs are not the main progenitors for the entire population of non-zero NCR SNe IIn, they may make up a sub-population of the progenitors.

## 5.5 The use of candidates in LBV studies

Our statistical tests show that candidate LBVs and confirmed LBVs are formally consistent, as far as their environments go. AD and WS tests comparing the NCR values of the two samples yield

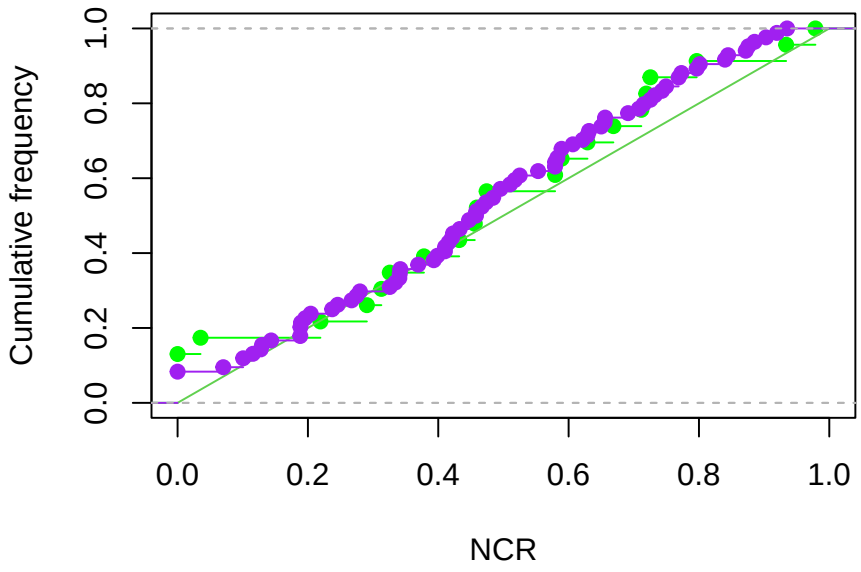


Figure 5.3: The empirical cumulative distribution of the confirmed (green) and candidate (purple) LBV samples plotted against a 1:1 NCR distribution.

p-values of 0.94 and 0.95, respectively. Additionally, their mean NCR values ($0.47 \pm 0.03$ for the confirmed and $0.46 \pm 0.03$ for the candidates) were within one error bar of each other, while their medians (0.46 for both) were similarly consistent. Therefore, confirmed LBVs and candidates are consistent with being drawn from the same parent distribution.

However, in spite of their formal consistency, the sample of confirmed LBVs was consistent with being drawn from the same NCR distribution as non-zero NCR SNe IIn via the AD test while the candidate sample was not. Additionally, although both samples rise above the p-value $< 0.05$ cutoff for consistency with being drawn from a uniform distribution with the WS test, the p-value for the candidates (0.091) was markedly lower than for the confirmed sample (0.32). The former suggests that the distribution of the candidate LBV sample may be distinct from the distribution of the non-zero NCR SNe IIn (if using a more generous 95% confidence interval), while the confirmed set is. Such a difference in results would support Humphreys et al. [42] in suggesting the use of

candidates in addition to confirmed LBVs in studies on the type can change the results of the study. This comes with a caveat that sampling size could account for the difference (with only 23 confirmed LBVs compared to 84 candidates in our sample), and the AD test (and all two-sample statistical tests) performing worse with smaller sample sizes. However, the difference in means and medians discussed lends some credibility to the possibility that the confirmed sample does follow a uniform NCR distribution, while the candidate sample, and thus also the combined sample, do not. This could suggest that the non-zero SNe IIn, which have been found to be consistent with a uniform distribution, may only share a parent distribution with the confirmed LBVs.

Additionally, comparing the radial distributions of the candidate and confirmed samples with AD and WS tests suggests that the distributions are distinct with a 95% confidence interval. This can be seen visually in the histograms in Figures 5.1a and 5.1b, where the distribution of contained R-band flux is visually distinct between the two samples. This is further evidence for the samples being statistically nonequivalent. However, this comes with the caveat that the number of confirmed LBVs usable for radial analysis was only 15 compared, making any type of statistical analysis risk being just small numbers statistics.

Based on our analysis, we propose that while the confirmed sample of LBVs may be a subset of the candidate sample, the candidate sample is not a subset of the confirmed sample. Or, even if every currently "un-confirmed" LBV could be identified as a candidate before an observed outburst, not every candidate would be an LBV. We present a few possibilities for the cause of this.

The most obvious possible cause for this would be simply that, in general, many young, massive stars look like LBVs, while only a very small percent of them are in actuality. This would likely be due to the very loose definition of "LBV candidates" that can change from paper to paper. The original description found in Bohannan [7] describes candidates as merely stars that may one day become LBVs, which leaves a wide range of interpretations for classification. In Smith & Tombleson [78], candidates are described as stars with similar luminosity and color as confirmed LBVs, which is broad enough to potentially lead to misidentification. The categorization issue is compounded by the ongoing debate into the exact mechanics of why LBVs have outbursts (see

Sections 1.3 and 1.4), which makes predicting which stars might eventually become an LBV (or is currently an LBV in quiescence), and subsequently the traits that cause it, difficult.

Another possibility is that, even if the majority of candidates do become LBVs in their lifetime, selection effects for candidates could change their makeup compared to that of confirmed LBVs. An example of this would be the focus in many studies on identifying candidates for classical, higher luminosity LBVs and ignoring potential lower-luminosity LBVs, potentially skewing the distribution of candidates compared to the total population of true LBVs.

The simplest explanation is that not all candidates are (or will become) LBVs, and this causes the observed differences. Therefore, we concur with Humphreys et al. [42] in recommending limited use of candidate LBVs when conducting studies of LBVs as a class. Unfortunately, this limits many studies to only using data from the few dozen confirmed LBVs (and a small fraction of those few dozen if the study can utilize only extra-galactic LBVs, like this one). Until more confirmed LBVs are discovered and observed, or a more rigorous method of accurately identifying "true" candidates is developed, studies of LBVs will be somewhat limited due to small sample size. In the future, large surveys, such as those to be conducted by the Large Synoptic Survey Telescope [45], can help expand the confirmed set.

## 5.6 Sources of error and future studies

A caveat often mentioned throughout this paper is the low sample size of confirmed LBVs. With fewer than 25 confirmed LBVs in our sample, it is still possible that our current sample may not be truly representative of the total LBV population. This is the main reason why candidate LBVs would be advantageous to use in a combined sample, as their numbers boosts the combined sample to over 80. However, our findings discussed in Section 5.5 suggest that there may be a large number of candidates that are not currently (or will not become) true LBVs. Thus, there appears to currently be no remedy for the problem of small sample size when studying extragalactic LBVs aside from discovering more genuine LBVs to observe in outburst or finding a reliable way to

accurately identify LBVs in quiescence and refine the candidate classification criteria.

Another consideration in our NCR analysis is the possibility of very small pockets of H$\alpha$ emission, low surface brightness H$\alpha$ emission, or dust obscured H$\alpha$ not detected in our exposures. While all the host galaxies analyzed are nearby ($z < 0.02$), compact star forming regions with diameters on the scale of 0.1 - 0.5 pc, such as those discussed in Churchwell [12] and Heydari-Malayeri et al. [36], might not be visible in some of our hosts. In this case, an LBV residing in one of these compact, or ultra-compact, SFR may have a recorded NCR of zero and thus not be considered to be in a SFR in our analysis. Additionally, the two hosts with the highest spatial resolutions in their pre-degraded exposures contain none of the zero-NCR confirmed LBVs, which may lend credence to the possibility of undetected H$\alpha$ regions in more distant or obscured hosts.

Future studies could focus on obtaining higher resolution images of the more distant galaxies and perform this pixel statistics method on less degraded images (although this loses the advantage of uniformity with previously conducted studies using the NCR method). Additionally, a future study could examine a possible NCR—R-band radial distribution of other massive, luminous stars like red supergiants, as suggested in Section 5.3. The NCR method could also be performed on other massive, luminous stars in nearby host galaxies to further explore their possible relations with LBVs.

# Chapter 6

# Conclusions

In this study, we have conducted the largest analysis of the environments of confirmed and candidate extra-galactic LBVs. Using the pixel-statistic method, we have examined how the distribution of LBVs follow H$\alpha$ emission, and thus ongoing SF. From our analysis, we find:

- Confirmed LBVs and candidate LBVs trace H$\alpha$ emission well, signifying they are well associated with regions of ongoing SF. This suggests that both sets are made up of short-lived, very luminous stars, which is consistent with the expected traits of the type in current literature. Our findings can neither support nor reject either a solely single-star evolution for the type or a binary evolution for the type due to limits of age estimates in this study.

- The NCR environments of confirmed LBVs and candidates are formally statistically consistent with being drawn from the same parent distribution according to the AD and WS tests. However, their radial distributions in their hosts in the R-band are statistically inconsistent with being drawn from the same parent distribution with a confidence interval of $>$ 95%. This suggests at least some population of stars that are not true LBVs in the candidate set. Because of this, we caution against using candidate LBVs to supplement the sample of confirmed LBVs in studies on the type.

- The non-zero NCR population of SNe IIn has a distribution consistent with that of confirmed LBVs, suggesting that LBVs do indeed make up a main population of non-zero NCR SNe IIn progenitors. Additionally, the radial distributions of the confirmed set and the combined set are both statistically consistent with being drawn from the same parent distribution as the non-zero SNe IIn. However, the NCR distribution of the candidate sample was found to be statistically inconsistent with the non-zero SNe IIn, supporting earlier findings that suggest the candidate and confirmed samples may be distinct sets.

Future studies yielding more confirmed and candidate LBVs will be greatly beneficial in learning more about these enigmatic stars.

# Acknowledgements

I'd like to first thank Dr. Conor Ransome, Dr. Abe Falcone, and Dr. Ashley Villar for all their help over the course of this project. I'd especially like to thank Conor for being a great mentor, both for this project and in general, over the past year and a half. I don't know how you managed to make it through dozens of meetings with me, but I am incredibly grateful for you support. I want to thank Abe for stepping in to be my thesis advisor after being asked at the very last minute. You have been a great source of knowledge throughout the project, and definitely saved me with my last-minute thesis proposal. And I'd like to thank Ashley, as without your support with the STAR program the project never would have happened.

I would also like to thank Dr. Phil Massey, who offered some great advice on the fool's errand of trying to stitch together a mosaic of M 31.

And finally, I would like to thank my family and my girlfriend, who have supported me throughout this project and my time in college. I wouldn't be where I am without you, and I want to especially thank you for bearing with me while I've been much too busy working on this.

# Bibliography

[1] Aadland E., Massey P., Neugent K. F., Drout M. R., 2018, The Astronomical Journal, 156, 294

[2] Abolmasov P., 2011, New Astronomy, 16, 421

[3] Aghakhanloo M., Murphy J. W., Smith N., Hložek R., 2017, Monthly Notices of the Royal Astronomical Society, 472, 591

[4] Anderson T. W., Darling D. A., 1954, Journal of the American statistical association, 49, 765

[5] Anderson J. P., Habergham S., James P., Hamuy M., 2012, Monthly Notices of the Royal Astronomical Society, 424, 1372

[6] Berger E., Foley R., Ivans I., 2009, The Astronomer's Telegram, 2184, 1

[7] Bohannan B., 1989, in International Astronomical Union Colloquium. pp 35–44

[8] Bothun G. D., Thompson I. B., 1988, Astronomical Journal (ISSN 0004-6256), vol. 96, Sept. 1988, p. 877-883., 96, 877

[9] Burgasser A., Nicholls C., Aberasturi M., 2012, The Astronomer's Telegram, 4431, 1

[10] Chugai N., 2001, Monthly Notices of the Royal Astronomical Society, 326, 1448

[11] Chugai N. N., et al., 2004, Monthly Notices of the Royal Astronomical Society, 352, 1213

[12] Churchwell E., 2002, Annual Review of Astronomy and Astrophysics, 40, 27

[13] Clark J., Larionov V., Arkharov A., 2005, Astronomy & Astrophysics, 435, 239

[14] Cohen J., 1992, Current directions in psychological science, 1, 98

[15] Cold C., Hjorth J., 2023, Astronomy & Astrophysics, 670, A48

[16] Collins K. A., Kielkopf J. F., Stassun K. G., Hessman F. V., 2017, The Astronomical Journal, 153, 77

[17] Conti P. S., 1984, in Symposium-International Astronomical Union. pp 233–254

[18] Crowther P. A., Willis A. J., 1993, Space science reviews, 66, 85

[19] Davidson K., Humphreys R. M., Weis K., 2016, arXiv preprint arXiv:1608.02007

[20] De Koter A., Lamers H., Schmutz W., 1996, Astronomy and Astrophysics, 306, 501

[21] De Paz A. G., Madore B., Pevunova O., 2003, The Astrophysical Journal Supplement Series, 147, 29

[22] De Vaucouleurs G., de Vaucouleurs A., Corwin J., 1976, Second reference catalogue of bright galaxies, 1976, 0

[23] Filippenko A. V., 1997, Annual Review of Astronomy and Astrophysics, 35, 309

[24] Gal-Yam A., Leonard D., 2009, Nature, 458, 865

[25] Gal-Yam A., et al., 2007, The Astrophysical Journal, 656, 372

[26] Gaustad J. E., McCullough P. R., Rosing W., Van Buren D., 2001, Publications of the Astronomical Society of the Pacific, 113, 1326

[27] Gogarten S. M., et al., 2009, The Astrophysical Journal, 691, 115

[28] Gräfener G., 2021, Astronomy & Astrophysics, 647, A13

[29] Gräfener G., Owocki S., Vink J., 2012, Astronomy & Astrophysics, 538, A40

[30] Groh J., Hillier D., Damineli A., Whitelock P., Marang F., Rossi C., 2009, The Astrophysical Journal, 698, 1698

[31] Groh J. H., Meynet G., Ekström S., 2013, Astronomy & Astrophysics, 550, L7

[32] Groh J. H., Meynet G., Ekström S., Georgy C., 2014, Astronomy & Astrophysics, 564, A30

[33] Habergham S., Anderson J., James P., Lyman J., 2014, Monthly Notices of the Royal Astronomical Society, 441, 2230

[34] Hallin M., Mordant G., Segers J., 2021, Electronic Journal of Statistics, 15, 1328

[35] Haydon D. T., Kruijssen J. D., Chevance M., Hygate A. P., Krumholz M. R., Schruba A., Longmore S. N., 2020, Monthly Notices of the Royal Astronomical Society, 498, 235

[36] Heydari-Malayeri M., Charmandaris V., Deharveng L., Rosa M., Schaerer D., Zinnecker H., 2001, Astronomy & Astrophysics, 372, 495

[37] Hoopes C. G., Walterbos R. A., 2000, The Astrophysical Journal, 541, 597

[38] Hoopes C. G., Walterbos R. A., Bothun G. D., 2001, The Astrophysical Journal, 559, 878

[39] Hubble E., Sandage A., 1953, Astrophysical Journal, vol. 118, p. 353, 118, 353

[40] Humphreys R. M., 1975, Astrophysical Journal, Vol. 200, p. 426-429, 200, 426

[41] Humphreys R. M., Davidson K., 1994, Publications of the Astronomical Society of the Pacific, 106, 1025

[42] Humphreys R. M., Weis K., Davidson K., Gordon M. S., 2016, The Astrophysical Journal, 825, 64

[43] Humphreys R. M., Gordon M. S., Martin J. C., Weis K., Hahn D., 2017, The Astrophysical Journal, 836, 64

[44] Humphreys R., Stangl S., Gordon M., Davidson K., Grammer S., 2019, VizieR Online Data Catalog, pp J–AJ

[45] Ivezić Ž., et al., 2019, The Astrophysical Journal, 873, 111

[46] James P., Anderson J., 2006, Astronomy & Astrophysics, 453, 57

[47] Jarrett T., Chester T., Cutri R., Schneider S., Huchra J., 2003, The Astronomical Journal, 125, 525

[48] Kangas T., et al., 2017, Astronomy & Astrophysics, 597, A92

[49] Kennicutt Jr R. C., 1998, Annual review of Astronomy and Astrophysics, 36, 189

[50] Kenyon S., Gallagher III J., 1985, The Astrophysical Journal, 290, 542

[51] Kiewe M., et al., 2011, The Astrophysical Journal, 744, 10

[52] King N., Walterbos R., Braun R., 1998, The Astrophysical Journal, 507, 210

[53] Knapen J., Stedman S., Bramich D., Folkes S., Bradley T., 2004, Astronomy & Astrophysics, 426, 1135

[54] Langer N., Hamann W.-R., Lennon M., Najarro F., Pauldrach A., Puls J., 1994, Astronomy and Astrophysics, 290, 819

[55] Massey P., 2006, The Astrophysical Journal, 638, L93

[56] Massey P., Olsen K., Hodge P. W., Strong S. B., Jacoby G. H., Schlingman W., Smith R., 2006, The Astronomical Journal, 131, 2478

[57] Massey P., Olsen K., Hodge P. W., Jacoby G. H., McNeill R. T., Smith R., Strong S. B., 2007a, The Astronomical Journal, 133, 2393

[58] Massey P., McNeill R. T., Olsen K., Hodge P. W., Blaha C., Jacoby G. H., Smith R., Strong S. B., 2007b, The Astronomical Journal, 134, 2474

[59] Massey P., Neugent K. F., Smart B. M., 2016, The Astronomical Journal, 152, 62

[60] Mauerhan J. C., et al., 2013, Monthly Notices of the Royal Astronomical Society, 430, 1801

[61] Mehner A., et al., 2021, Astronomy & Astrophysics, 655, A33

[62] Moriya T. J., Maeda K., 2014, The Astrophysical Journal Letters, 790, L16

[63] Neugent K. F., Massey P., 2011, The Astrophysical Journal, 733, 123

[64] Nilson P., 1973, Nova Acta Regiae Soc. Sci. Upsaliensis Ser. V, p. 0

[65] Pearson K., 1895, Proceedings of the Royal Society of London Series I, 58, 240

[66] Petrovic J., Pols O., Langer N., 2006, Astronomy & Astrophysics, 450, 219

[67] Price-Whelan A. M., et al., 2022, The Astrophysical Journal, 935, 167

[68] Ransome C., Habergham-Mawson S., Darnley M., James P., Filippenko A., Schlegel E., 2021, Monthly Notices of the Royal Astronomical Society, 506, 4715

[69] Ransome C. L., Habergham-Mawson S., Darnley M. J., James P. A., Percival S. M., 2022, Monthly Notices of the Royal Astronomical Society, 513, 3564

[70] Razali N. M., Wah Y. B., et al., 2011, Journal of statistical modeling and analytics, 2, 21

[71] Salamanca I., Terlevich R. J., Tenorio-Tagle G., 2002, Monthly Notices of the Royal Astronomical Society, 330, 844

[72] Sana H., et al., 2012, Science, 337, 444

[73] Sandage A., Tammann G., 1974, Astrophysical Journal, Vol. 191, p. 603-621, 191, 603

[74] Schlegel E. M., 1990, Monthly Notices of the Royal Astronomical Society, 244, 269

[75] Skrutskie M. F., et al., 2006, The Astronomical Journal, 131, 1163

[76] Smith N., 2017, Philosophical Transactions of the Royal Society A: Mathematical, Physical and Engineering Sciences, 375, 20160268

[77] Smith N., Gehrz R. D., 1998, The Astronomical Journal, 116, 823

[78] Smith N., Tombleson R., 2015, Monthly Notices of the Royal Astronomical Society, 447, 598

[79] Solovyeva Y., Vinokurov A., Kostenkov A., Sarkisyan A., Atapin K., Valeev A., 2021, arXiv preprint arXiv:2109.05891

[80] Springob C. M., Haynes M. P., Giovanelli R., Kent B. R., 2005, The Astrophysical Journal Supplement Series, 160, 149

[81] Stanek K., Garnavich P., 1998, The Astrophysical Journal, 503, L131

[82] Van Genderen A., 2001, Astronomy & Astrophysics, 366, 508

[83] Van Genderen A., Sterken C., 2002, Astronomy & Astrophysics, 386, 926

[84] Vink J. S., de Koter A., 2002, Astronomy & Astrophysics, 393, 543

[85] Virtanen P., et al., 2020, Nature Methods, 17, 261